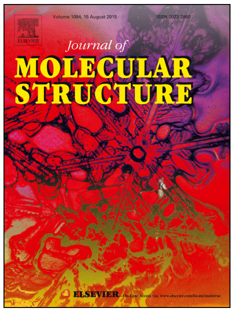

A new chromenylium-cyanine chemosensor for switch-ON near-infrared copper (II) sensing

Kaan Karaoglu

PII: S0022-2860(19)31749-1

DOI: https://doi.org/10.1016/j.molstruc.2019.127640

Reference: MOLSTR 127640

To appear in: *Journal of Molecular Structure*

Received Date: 24 October 2019

Revised Date: 20 December 2019

Accepted Date: 22 December 2019

Please cite this article as: K. Karaoglu, A new chromenylium-cyanine chemosensor for switch-ON near-infrared copper (II) sensing, *Journal of Molecular Structure* (2020), doi: https://doi.org/10.1016/j.molstruc.2019.127640.

Kaan KARAOGLU: Conceptualization, Methodology, Validation, Investigation.

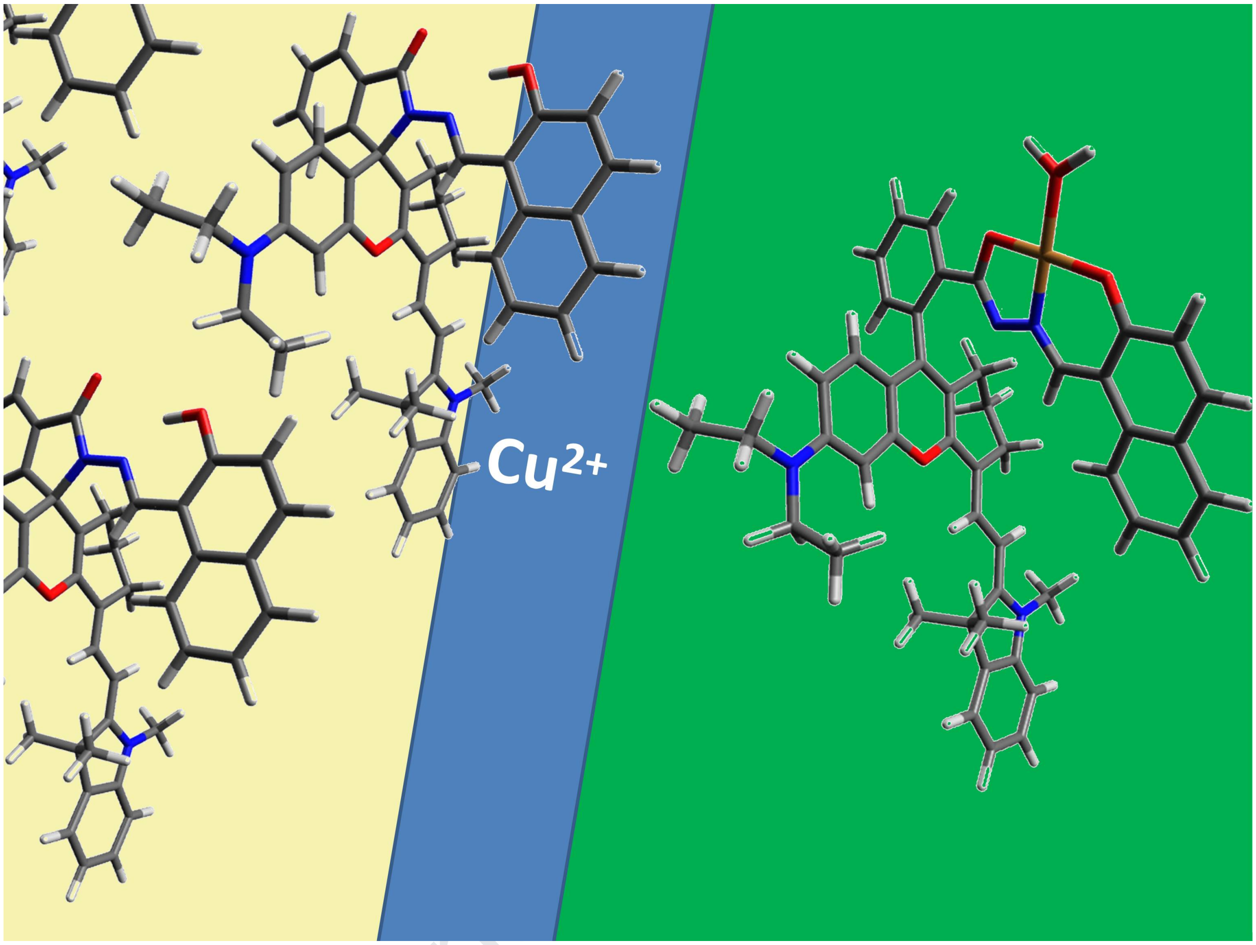
Cu2+

A new chromenylium-cyanine chemosensor for switch-ON near-infrared copper (II) sensing

Kaan KARAOGLU[1*]

[1] Department of Chemistry and Chemical Process Technology, Vocational School of Technical Sciences, Recep Tayyip Erdogan University, Rize, TURKEY

*Correspondence: kaan.karaoglu@erdogan.edu.tr

ORCID:

Kaan KARAOGLU: https://orcid.org/0000-0003-3265-8328

Abstract: A highly selective and sensitive near-IR chemosensor having a chromenylium-cyanine backbone for the detection of Cu^{2+} in aqueous samples has been designed and synthesized. The sensor has exhibited linear optical response to copper ions at the range of $0–4.9\times10^{-6}$ M in the presence of other competing metal ions, such as Na^+, K^+, Mg^{2+}, Ca^{2+}, Cr^{3+}, Mn^{2+}, Fe^{3+}, Co^{2+}, Ni^{2+}, Zn^{2+}, Al^{3+}, Cd^{2+}, Ag^+, Sr^{2+}, Pb^{2+}, Hg^{2+} and Ba^{2+}. The limit of detection (LOD) was calculated as 1.28×10^{-8} M which was lower than that of previously reported analogues. The sensor allows detection of the copper(II) ion through the spirocyclic ring-opening reaction by coordination of Cu^{2+}.

Key words: Near-IR chemosensor, copper sensing, chromenylium-cyanine

1. Introduction

In the last couple of decades, there has been a growing interest in design of ion-selective colorimetric sensors owing to their potential applications, such as tissue imagining [1], online environmental monitoring [2], investigation of cellular events [3] and even in aerospace technology [4]. Xanthene dyes are one of the most studied classes of compounds thanks to their optical properties, such as high molar absorptivity, high fluorescence quantum yields and relatively simple preparation procedures. Xanthenes enable ion sensing by colour change from colourless to pink associated with spirolactam ring opening through coordination or irreversible reactions [5,6].

The permitted limit of copper in drinking water has been established as 20 μM by the U.S. Environmental Protection Agency (EPA) [7]. A series of rhodamine B Schiff-base derivative-sensors have been synthesized, and their copper sensing properties have been also investigated [8–11]. Although these sensors have effectively detected the ion content of analysis media, the main disadvantages of rhodamine B Schiff-bases are lower tissue penetration, photodamage to biomolecules and photoscattering in in vivo cell imagining. Thus, new copper sensors – having higher selectivity and sensitivity toward copper ions – have attracted increasing attention due their potential applications in biomolecular monitoring functions. In the last decade, chromenylium-cyanine fluorophore (CC-Fluor) sensors have facilitated online monitoring of metal ions lying in the NIR region (620−760 nm) [12].

In this study, a new chromenylium-cyanine near-IR fluorescent probe was designed and characterized for selective and sensitive determination of Cu^{2+} in aqueous solutions. The selectivity and sensitivity of the sensor have been investigated in a group of metal ions containing Na^{+}, K^{+}, Mg^{2+}, Ca^{2+}, Cr^{2+}, Mn^{2+}, Fe^{3+}, Co^{2+}, Ni^{2+}, Cu^{2+}, Zn^{2+}, Al^{3+}, Ag^{+}, Cd^{2+}, Sr^{2+} Hg^{2+}, Pb^{2+} and Ba^{2+}, and analytical data have been compared with studies that produced similar molecular structures [6,13]. A chromenylium-cyanine derivative was found to be highly selective and sensitive to Cu^{2+} among other metal ions at the near-IR region.

2. Experimental

3-Diethylaminohenol, phthalic anhydride, hydrazine hydrate and (benzotriazol-1-yloxy)tris(dimethylamino)phosphonium hexafluorophosphate were obtained from Sigma Aldrich and cyclohexanone were obtained from TEKKIM, a local supplier from Turkey. The solvents used in chromatography were of reagent grade and used without further purification – except for ethanol, which was dried over molecular sieve type 4A. Metal ion solutions, Na^+, K^+, Mg^{2+}, Ca^{2+}, Cr^{2+}, Fe^{3+}, Co^{2+}, Ni^{2+}, Cu^{2+}, Zn^{2+}, Al^{3+}, Ag^+, Cd^{2+}, Sr^{2+} Hg^{2+}, Pb^{2+} and Ba^{2+}, were prepared freshly from their nitrate salts, except for Mn^{2+}, which was prepared from acetate salt.

2.1. Synthesis of sensor

(4'Z)-2-amino-6'-(diethylamino)-4'-{2-[(2Z)-1,3,3-trimethyl-2,3-dihydro-1H-indol-2-yl den]ethyliden}-1',2,2',3,3',4'-hexahydrospiro[isoindol-1,9'-xanthene]-3-on was synthesized by following the synthetic route described in Figure 1 [6,14]. Compound **4** (0.573 g, 1 mmol) was dissolved in absolute ethanol and solution purged by argon for 30 min. Then, 2-hydroxy-1-naphthaldehyde (1.1 mmol) was added into the solution and the mixture was stirred at ambient temperature for 48 h. The solvent was evaporated by rotary under reduced pressure, and the crude product was purified by chromatography (Rf: 0.57, EtOH/CH_2Cl_2, 1:20, v/v). Colour: Yellow. Yield: 26%. Analytical data for C_{48} $H_{46}N_4O_3$, ESI-MS (m/z) 726 $[M+H]^+$ (726.90 calc.). ^1H NMR data (500 Mhz, $CDCl_3$) δ, ppm: 1.160 (t, J= 7.0 Hz, 6H), 1.385 (s, 1H), 1.633–1.609 (m, 3H), 1.795 (s, 3H), 1.824 (s, 3H), 3.148 (s, 3H), 3.333 (q, J=7.5 Hz, 4H), 5.387 (d J=12.5 Hz, 1H); 6.286 (d, J=8.5 Hz, 1H), 6.449 (s, 1H), 6.500 (d, J= 9.0 Hz), 6.634 (d, J=8.0 Hz, 1H), 6.879 (t, J=7.5 Hz, 1H), 7.166 (d, J=6.5 Hz, 1H), 7.147 (d, J=6.0 Hz, 1H), 7.210 (t, J=6.5 Hz, 1H), 7.452 (t, J=8.0 Hz, 1H), 7.521 (t, J=7.5 Hz, 1H), 7.587 (t, 7.5 Hz, 1H), 7.637 (t, J= 6.0 Hz, 1H), 7.700 (dd, J= 8.5Hz, j= 3.5 Hz, 2H), 7.819 (d, J=8.0 Hz, 1H), 7.908 (d, J=8.5 Hz, 1H), 8.001 (d, J=8.5 Hz, 1H), 8.370 (d, J=8.5 Hz, 1H), 9.685 (s, 1H), 10.838 (s, 1H). ^{13}C NMR data (126 Mhz, $CDCl_3$) δ, ppm: 12.252, 22.079, 23.010, 28.382, 28.473, 29.122, 44.334, 45.506, 67.849, 92.147, 97.562, 103.170, 104.460, 105.735, 108.701, 108.986, 118.606, 119.194, 119.873, 120.364, 121.542, 123.084, 123.521, 124.513, 127.157, 127.731, 127.989, 128.058, 128.765, 129.141, 129.493, 129.677, 132.443, 132.511, 133.391, 138.837, 139.180, 145.346, 146.522, 149.043, 152.398, 158.851, 164.378.

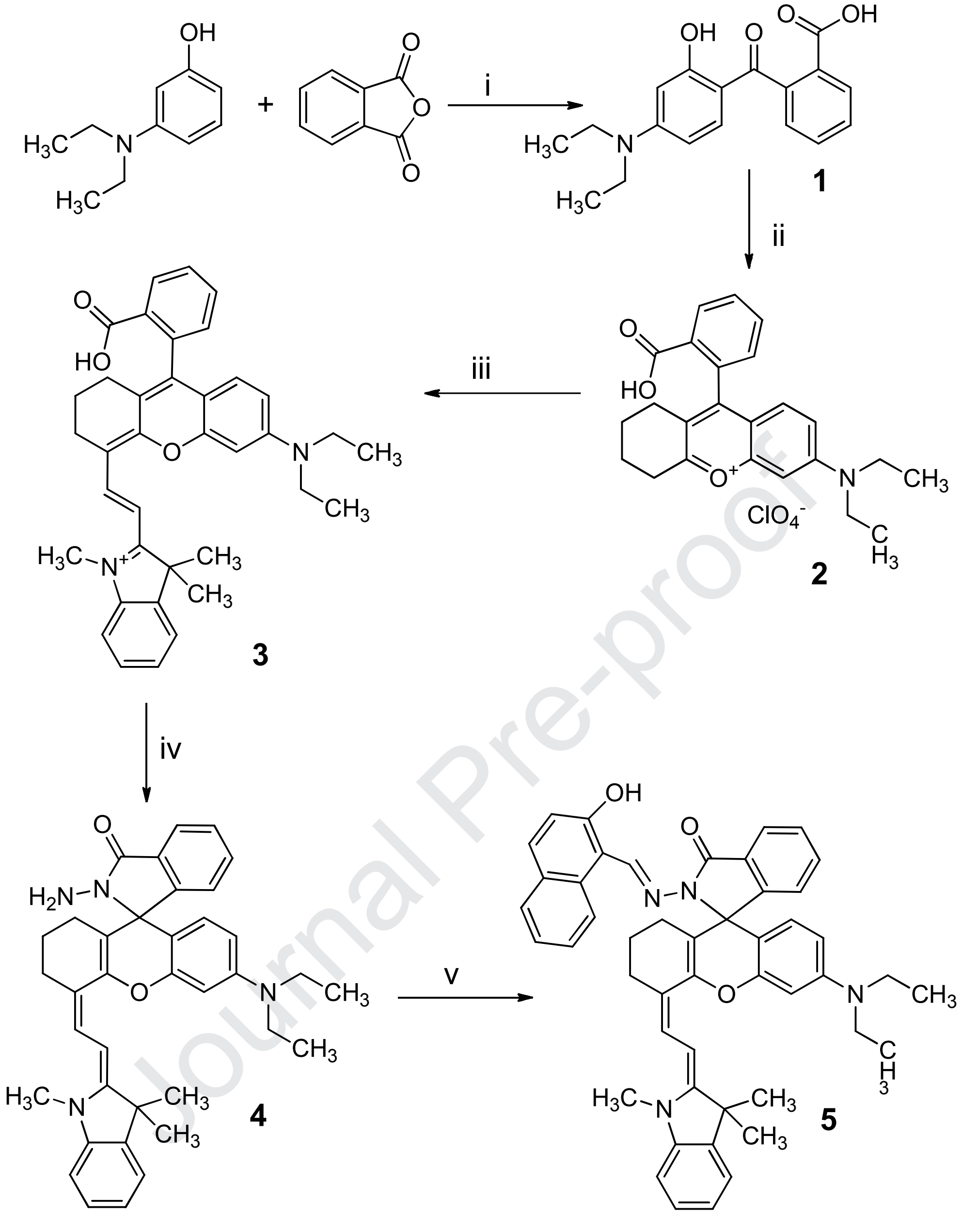

Figure 1. Synthesis scheme of the sensor. i: Toluene, 3h, 35% NaOH, 10,0 M HCl; ii: H_2SO_4, cyclohexanone, 2h; iii: 2-(1,3,3-trimethylindolin-2-ylden)acetaldehyde; iv: hydrazin hydrate, BOP reagent; v: 2-hydroxy-1-naphthaldehyde.

2.2. Spectrophotometric assays

In typical metal sensing analysis, 1×10^{-3} M nitric acid (1.0%) solutions of the metal ions, Na^+, K^+, Mg^{2+}, Ca^{2+}, Cr^{2+}, Mn^{2+}, Fe^{3+}, Co^{2+}, Ni^{2+}, Cu^{2+}, Zn^{2+}, Al^{3+}, Ag^+, Cd^{2+}, Sr^{2+}

Hg^{2+}, Pb^{2+} and Ba^{2+}, were prepared from their nitrate salts, except for Mn^{2+}, which was prepared from acetate. In selectivity experiments, a 1×10^{-5} M sensor in 100 mM tris/nitrate buffer (ethanol/water, 2:1, v/v) and 5 eq. each of metal ion were incubated for 5 minutes, at which point spectrophotometric measurements were performed at the visible region. The selectivity of the sensor as a colorimetric chemosensor for the detection of Cu^{2+} was also studied in the presence of various competing metal cations. In a competition experiment, a series sensor solution was treated with mixtures containing equimolar amounts of Cu^{2+} and competitive ions.

The detection limit of the sensor based on standard deviation of the blank measurements by The International Union of Pure and Applied Chemistry (IUPAC) was determined from Eq. (1).

$$LOD = \frac{3\times Sd}{S} \tag{1}$$

Where Sd is the standard deviation of the intercept that is calculated by regression analysis at the 95% confidence level, and S is the slope of the calibration curve.

3. Results and discussion

3.1. Characterization

The chemical structure of the sensor was characterized by spectroscopic methods, such as FTIR, ^{1}H and ^{13}C NMR, UV/vis and mass spectrometry. The FT-IR spectrum of sensor is given in Figure S. 1. Phenolic –OH stretching was observed at 3292 cm^{-1}, and asymmetric and symmetric C–H stretching modes for sp^3 hybridized carbon atoms were observed at 2964 and 2926 cm^{-1}, respectively. Signals detected at 1690 cm^{-1} and 1620 cm^{-1} correspond to carbonyl and imine stretching modes of spirocycle, respectively. The disappearance of the carbonyl band and the shift of the imino stretching to 1616 cm^{-1}

clearly suggest the formation of the ring-opened amide form of the sensor as a result of Cu^{2+} coordination (Figure S. 2 and Figure S. 3). The chemical structure of the sensor was confirmed by NMR spectra, with the atoms labelled as shown in Figure S. 4 and Figure S. 5. Signals corresponding to CH_3 protons were detected as singlets at 3.148, 1.824 and 1.795 ppm for H_{53}, H_{54} and H_{55}, respectively. A triplet signal has been observed at 1.160 ppm (J=7.0 Hz), corresponding to 6H (H_{38} and H_{52}). N-substituted CH_2 signals for H_{37} and H_{51} have been observed as a quartet at 3.333 ppm (J= 7.5 Hz). CH_2 signals belonging to the chromenylium ring system gave three sets of signals: H_{20}, H_{23} and one of the H_{21}. The other proton signal of H_{21} were observed as a singlet at 1.385 ppm, because of non-planar structure of ring system (for detailed information, see the theoretical calculations section) [15]. The signals of the imine proton and phenolic –OH functional were observed at 9.685 and 10.838 ppm, respectively. The characteristic ^{13}C NMR signals of carbonyl (C6) and the C4 corresponding spirocycle closed form were observed at 164.378 and 67.849 ppm, respectively (Figure S. 6 and Figure S. 7) [16]. Mass spectra of the sensor and its copper complex were also analysed by H-ESI mass spectrometry. The peaks corresponding to the molecular ion and its sodium adduct were observed at 726.25 and 748.50 m/z, respectively (for isotope distribution, see Figure S. 8). The molecular ion peaks for copper complex with coordinated methanol molecule were observed at 821.97 m/z in H-ESI mass spectra (Figure S. 9).

3.2. Selectivity of the sensor

The selectivity and sensitivity of the similar structure derived from rhodamine B hydrazide bearing 2-hydroxy-1-naphthaldehyde have been previously investigated, and it was found that this derivative showed an optical signal toward Cu^{2+}, Hg^{2+} and Mg^{2+}

[6,13]. The selectivity of the chromenylium-cyanine based sensor was investigated in an ethanol/tris-nitrate buffer (2:1, v/v, pH 7.02) with various metal ions such as Na^+, K^+, Mg^{2+}, Ca^{2+}, Cr^{2+}, Mn^{2+}, Fe^{3+}, Co^{2+}, Ni^{2+}, Cu^{2+}, Zn^{2+}, Al^{3+}, Ag^+, Cd^{2+}, Sr^{2+} Hg^{2+}, Pb^{2+} and Ba^{2+}. While the other metal ions had a negligible response, the solution turned from pale yellow to green upon addition of Cu^{2+} to a solution of the sensor, and the absorbance was significantly enhanced, with a new peak located at 710 nm (Figure 2).

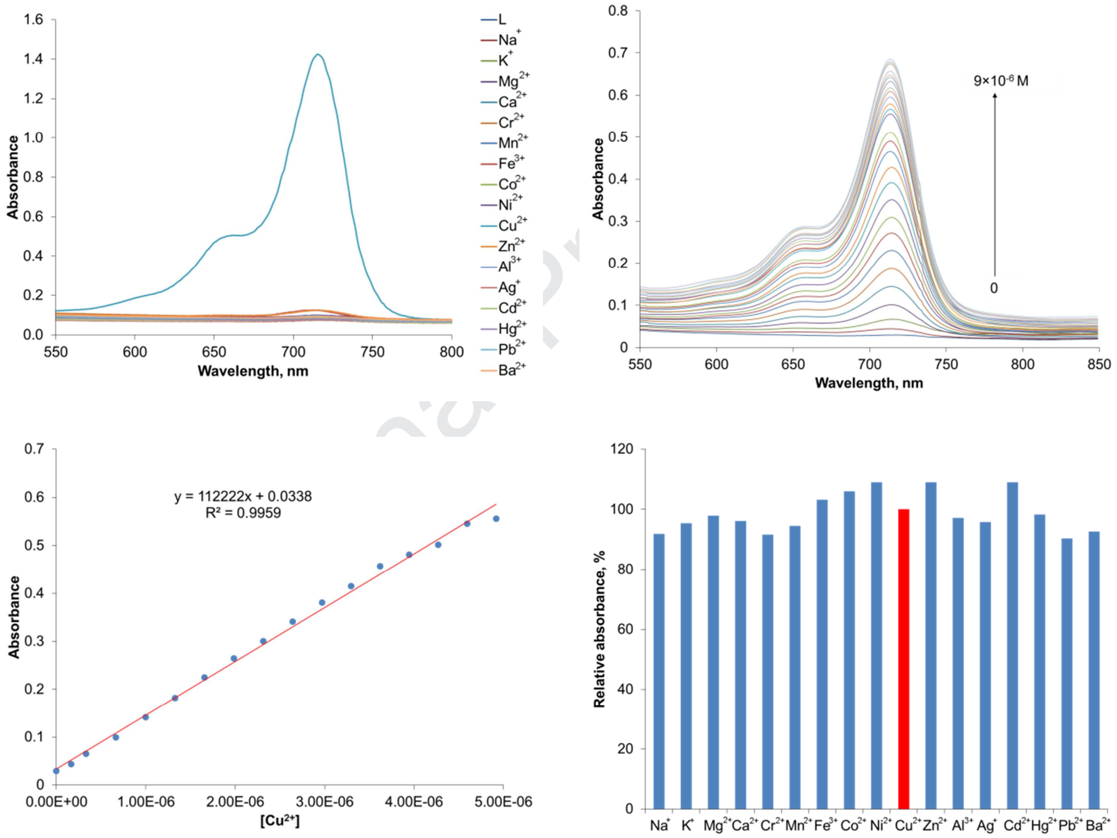

Figure 2. Changes in absorption spectra of sensor (10 μM) in ethanol/Tris–nitrate buffer (2:1, v/v, pH 7.02) solutions – presence of 5.0×10^{-5} M metal ions (upper left), with various amounts of Cu^{2+} ions ($0\text{-}9.0\times10^{-6}$ M, upper right), linear working curve derived from titration with Cu^{2+} at 710 nm (lower left) and optical response of sensor to Cu^{2+} ion among competitive metal ions.

Titration experiments showed that the sensor generates an optical signal as a function of increasing Cu^{2+} ion having linearity from 0 to 4.9×10^{-6} M. The LOD value for the sensor toward the Cu^{2+} ion by colorimetry was calculated as 1.28×10^{-8} M by the linear working curve. It has previously been observed that a similar Schiff base structure having a xanthene ring backbone showed selectivity toward Hg^{2+} and Cu^{2+} ions at 558 nm with and a LOD value of 2.0×10^{-7} M [6].

In order to investigate the selectivity of the sensor in the presence of competitive mono-, di- and trivalent metal ions such as Na^{+}, K^{+}, Mg^{2+}, Ca^{2+}, Cr^{2+}, Mn^{2+}, Fe^{3+}, Co^{2+}, Ni^{2+}, Zn^{2+}, Al^{3+}, Ag^{+}, Cd^{2+}, Sr^{2+} Hg^{2+}, Pb^{2+} and Ba^{2+}, the experiments were conducted by an addition of 1.0 equivalent of Cu^{2+} to solutions containing 2.0 equivalent of other metal ions in the same media. The selectivity experiments showed that – as seen in Figure 2 – none of the competitive metal ions had obvious interference with the detection of Cu^{2+}. This suggests that the sensor complex could selectively distinguish Cu^{2+} ions from the competing metal ions through the naked eye in ethanol/water mixtures (2:1, v/v) at pH 7.02.

3.3. Theoretical calculations

The molecular structure of the sensor and its copper(II) complex in the gas phase have been investigated by density functional theory (DFT) using the Becke-3-Lee-Yang-Parr (B3LYP) exchange-correlation functional with a 6-31G(d, p) basis set for the H, C, N and O and LanL2Dz for the Cu atom [17,18]. Geometric structures, vibration frequencies and vertical excitation energies have been investigated by the GAMESS 2018 program [19], and computational data were visualized by Gabedit [20]. The positive values of all calculated vibrational wavenumbers show that the optimized molecular structures are stable at a minimum on the potential energy surface. The lowest 10 singlet-singlet transitions of the sensor and 5 of its copper complex have been calculated by time-dependent DFT (TD-DFT) formalism.

The DFT-optimized geometries of the sensor and its copper complex are given in Figure 3. DFT calculations showed that the nitrogen atom of the N,N-diethyl amino unit bounded to the chromenylium ring has a trigonal planar structure, and this data confirms that the group is conjugated with the chromenylium ring system [21]. Because of angle strain, the cyclic ring fused in chromenylium ring has an eclipsed conformation in which two axial (C–H_{20a} and C–H_{22a}) and three equatorial (C–H_{20b}, C–H_{21a} and C–H_{22b}) bonds lie in almost one side of ring. Since the direction of C–H_{21b} is on the other side of the ring, the chemical environment of this proton changes dramatically, resulting in the ^{1}H NMR signal observed as a singlet in the upper field with respect to the adjacent protons (see Figure S. 10).

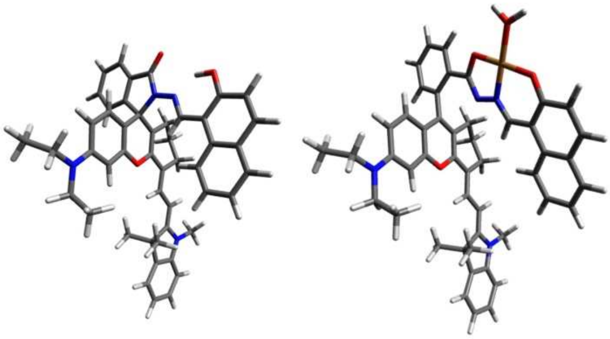

Figure 3. DFT optimized structures of sensor (left) and its copper complex (right).

UV/vis. spectrum of the sensor and its copper complex were recorded at room temperature (see Figure S. 11). TD-DFT calculations showed that the shoulder located at 426 nm in experimental UV/vis. spectrum (calc. 443 nm) corresponds to the HOMO→LUMO transition; and the peak located at 371 nm (calc. 368 nm) corresponds to the HOMO→LUMO+1 transition (for detailed spectral analysis, see Supplementary File, Figure S.12). These electronic excitations are mainly contributed by $\pi \rightarrow \pi^*$ transitions from 1,3,5-alkatrien to Schiff base through spirocycle (Figure 4). TD-DFT calculations also showed that E_{HOMO} and E_{LUMO} of the sensor are -4.53 eV and -1.32 eV, respectively. The experimental electronic spectrum and the calculated data, as well as the optical energy gap (E_g^{opt}), are in accordance with closed-form of the spirocycle ring system.

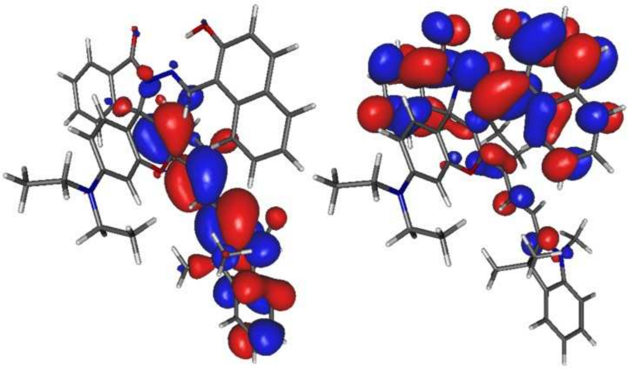

Figure 4. HOMO (left) and LUMO (right) orbitals of the sensor (isovalue set to 0.02 a.u.)

It was suggested that the complex has the ring-opened amide form as a result of the coordination of copper through the oxygen atom of carbonyl and the nitrogen atom of imino moiety, which would be consistent with previously reported findings [6,22]. The calculated geometry of reported complex by DFT showed that copper centre has square planar geometry with a D–Cu–D bond angle (D represents donor atoms) of 90.04±6.07º and a D–Cu–D dihedral angle of 176.2±0.8º. TD-DFT calculations showed that HOMO was delocalized on Schiff base parts, while the LUMO was delocalized over the chromenylium unit with a calculated HOMO–LUMO gap of 2.19 eV (Figure 5).

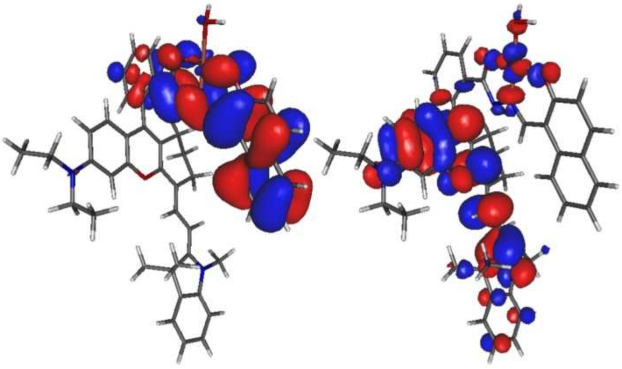

Figure 5. HOMO (left) and LUMO (right) orbitals of the copper(II) complex of sensor (isovalue set to 0.02 a.u.)

The band observed at 710 nm in experimental UV/vis. spectrum consists of two transitions, HOMO→LUMO and HOMO→LUMO+1. While the calculated HOMO→LUMO transition was mainly contributed to by π→π* transitions, the HOMO→LUMO+1 transition was assigned to a ligand to metal charge transfer (LMCT) band (Figure S. 13). The calculated energy gap for the sensor and its copper(II) complex is also clearly shown in the density of states (DOS) plot (Figure S. 14). The TD-DFT method has been used to evaluate the electronic structure of the investigated compounds, and strong correlations have been noted between the experimental and calculated data.

4. Conclusion

In summary, this study reported the synthesis, characterization and sensing properties of the chromenylium-cyanine sensor by colorimetric measurements. The spectrophotometric experiments showed that the sensor enables selective and sensitive recognition of the Cu^{2+} ion in the near-IR region over competitive mono-, di- and trivalent metal ions, such as Na^{+}, K^{+}, Mg^{2+}, Ca^{2+}, Cr^{2+}, Mn^{2+}, Fe^{3+}, Co^{2+}, Ni^{2+}, Cu^{2+}, Zn^{2+}, Al^{3+}, Ag^{+}, Cd^{2+}, Sr^{2+} Hg^{2+}, Pb^{2+} and Ba^{2+}. The LOD value for the sensor toward Cu^{2+} was calculated as 1.28×10^{-8} M based on standard deviation of the blank measurements by IUPAC. As a result of the complex formation with the Cu^{2+} ion, optical absorption at near-IR region is expected to be generated by a spirolactam ring opening reaction. The optimized geometries and the electronic structure of the compounds have been investigated by DFT, and a strong correlation has been noted between the theoretical and experimental data. Spectrophotometric analysis showed that there is a significant decrease in the detection limit compared to the xanthene derivative in existing scholarship, the synthesized sensor showed higher selectivity toward the copper(II) ion, which makes it possible to perform the analysis in the near-IR region.

Acknowledgment

The numerical calculations reported in this paper were fully performed at TUBITAK ULAKBIM, High Performance and Grid Computing Center (TRUBA resources).

References

[1] J.Y. Xie, C.Y. Li, Y.F. Li, Y.J. Fu, S.X. Nie, H.Y. Tan, A near-infrared chemosensor for determination of trivalent aluminum ions in living cells and tissues, Dye. Pigment. 136 (2017) 817–824. https://doi.org/10.1016/j.dyepig.2016.09.046.

[2] Ö. Şahin, M. Şahin, N. Koçak, M. Ylmaz, A new anthracene derivative of calix[4]arene as a fluorescent chemosensor, Turk. J. Chem. 37 (2013) 832–839. https://doi.org/10.3906/kim-1302-77.

[3] S. Zhang, T.H. Chen, H.M. Lee, J. Bi, A. Ghosh, M. Fang, Z. Qian, F. Xie, J. Ainsley, C. Christov, F.T. Luo, F. Zhao, H. Liu, Luminescent probes for sensitive detection of ph changes in live cells through two near-infrared luminescence channels, ACS Sensors. 2 (2017) 924–931. https://doi.org/10.1021/acssensors.7b00137.

[4] O.S. Wolfbeis, Materials for fluorescence-based optical chemical sensors, J. Mater. Chem. 15 (2005) 2657. https://doi.org/10.1039/b501536g.

[5] S. Kenmoku, Y. Urano, H. Kojima, T. Nagano, Development of a highly specific rhodamine-based fluorescence probe for hypochlorous acid and its application to real-time imaging of phagocytosis., J. Am. Chem. Soc. 129 (2007) 7313–7318. https://doi.org/10.1021/ja068740g.

[6] M. Dong, T.H. Ma, A.J. Zhang, Y.M. Dong, Y.W. Wang, Y. Peng, A series of highly sensitive and selective fluorescent and colorimetric “off-on” chemosensors for Cu (II) based on rhodamine derivatives, Dye. Pigment. 87 (2010) 164–172. https://doi.org/10.1016/j.dyepig.2010.03.015.

[7] L. Li, S. Shen, R. Lin, Y. Bai, H. Liu, Rapid and specific luminescence sensing

of Cu(II) ions with a porphyrinic metal–organic framework, Chem. Commun. 53 (2017) 9986–9989. https://doi.org/10.1039/C7CC04250G.

[8] H.N. Kim, M.H. Lee, H.J. Kim, J.S. Kim, J. Yoon, A new trend in rhodamine-based chemosensors: application of spirolactam ring-opening to sensing ions., Chem. Soc. Rev. 37 (2008) 1465–72. https://doi.org/10.1039/b802497a.

[9] S. Park, W. Kim, K.M.K. Swamy, H.Y. Lee, J.Y. Jung, G. Kim, Y. Kim, S.-J. Kim, J. Yoon, Rhodamine hydrazone derivatives bearing thiophene group as fluorescent chemosensors for Hg^{2+}, Dye. Pigment. 99 (2013) 323–328. https://doi.org/10.1016/j.dyepig.2013.05.015.

[10] K. Wechakorn, K. Suksen, P. Piyachaturawat, P. Kongsaeree, Rhodamine-based fluorescent and colorimetric sensor for zinc and its application in bioimaging, Sensors Actuators, B Chem. 228 (2016) 270–277. https://doi.org/10.1016/j.snb.2016.01.045.

[11] K. Wechakorn, S. Prabpai, K. Suksen, P. Kanjanasirirat, Y. Pewkliang, S. Borwornpinyo, P. Kongsaeree, A rhodamine-triazole fluorescent chemodosimeter for Cu^{2+} detection and its application in bioimaging, Luminescence. 33 (2018) 64–70. https://doi.org/10.1002/bio.3373.

[12] Y. Wei, D. Cheng, T. Ren, Y. Li, Z. Zeng, L. Yuan, Design of NIR Chromenylium-Cyanine Fluorophore Library for “Switch-ON” and Ratiometric Detection of Bio-Active Species In Vivo, Anal. Chem. 88 (2016) 1842–1849. https://doi.org/10.1021/acs.analchem.5b04169.

[13] Y. Zhao, B. Zheng, J. Du, D. Xiao, L. Yang, A fluorescent “turn-on” probe for the dual-channel detection of Hg(II) and Mg(II) and its application of imaging in living cells, Talanta. 85 (2011) 2194–2201.

https://doi.org/10.1016/j.talanta.2011.07.070.

[14] Q.-H. Liu, X.-L. Yan, J.-C. Guo, D.-H. Wang, L. Li, F.-Y. Yan, L.-G. Chen, Spectrofluorimetric determination of trace nitrite with a novel fluorescent probe, Spectrochim. Acta Part A Mol. Biomol. Spectrosc. 73 (2009) 789–793. https://doi.org/10.1016/j.saa.2009.03.018.

[15] G.K. Vegesna, J. Janjanam, J. Bi, F.T. Luo, J. Zhang, C. Olds, A. Tiwari, H. Liu, PH-activatable near-infrared fluorescent probes for detection of lysosomal pH inside living cells, J. Mater. Chem. B. 2 (2014) 4500–4508. https://doi.org/10.1039/c4tb00475b.

[16] S. Zhang, T.-H. Chen, H.-M. Lee, J. Bi, A. Ghosh, M. Fang, Z. Qian, F. Xie, J. Ainsely, C.Z. Christov, F.-T. Luo, F. Zhao, H. Liu, Luminescent Probes for Sensitive Detection of pH Changes in Live Cells through Two Near-infrared Luminescence Channels, ACS Sensors. (2017) acssensors.7b00137. https://doi.org/10.1021/acssensors.7b00137.

[17] A.D. Becke, A new mixing of Hartree–Fock and local density-functional theories, J. Chem. Phys. 98 (1993) 1372. https://doi.org/10.1063/1.464304.

[18] P.C.C. Hariharan, J.A. a. Pople, The influence of polarization functions on molecular orbital hydrogenation energies, Theor. Chim. Acta. 28 (1973) 213–222. https://doi.org/10.1007/BF00533485.

[19] M.W. Schmidt, K.K. Baldridge, J.A. Boatz, S.T. Elbert, M.S. Gordon, J.H. Jensen, S. Koseki, N. Matsunaga, K.A. Nguyen, S. Su, T.L. Windus, M. Dupuis, J.A. Montgomery, General atomic and molecular electronic structure system, J. Comput. Chem. 14 (1993) 1347–1363. https://doi.org/10.1002/jcc.540141112.

[20] A.-R. Allouche, Gabedit-A graphical user interface for computational chemistry

softwares, J. Comput. Chem. 32 (2011) 174–182. https://doi.org/10.1002/jcc.21600.

[21] Z. Xu, L. Zhang, R. Guo, T. Xiang, C. Wu, Z. Zheng, F. Yang, A highly sensitive and selective colorimetric and off-on fluorescent chemosensor for Cu2+ based on rhodamine B derivative, Sensors Actuators, B Chem. 156 (2011) 546–552. https://doi.org/10.1016/j.snb.2011.01.066.

[22] N. LI, C. YU, Y. JI, J. ZHANG, Characterization of a Cu^{2+}-selective fluorescent probe derived from rhodamine B with 1,2,4-triazole as subunit and its application in cell imaging, Turk. J. Chem. 39 (2015) 660–666. https://doi.org/10.3906/kim-1410-58.

- A new chromenylium-cyanine sensor was designed for coper(II) ion sensing in aqueous media.
- The sensor allows detection of the copper (II) ion through the spirocyclic ring-opening reaction by coordination of Cu^{2+}.
- The sensor showed selectivity to copper ion in the presence of competitive mono-, di- and trivalent metal ions such as Na^{+}, K^{+}, Mg^{2+}, Ca^{2+}, Cr^{2+}, Mn^{2+}, Fe^{3+}, Co^{2+}, Ni^{2+}, Zn^{2+}, Al^{3+}, Ag^{+}, Cd^{2+}, Sr^{2+} Hg^{2+}, Pb^{2+} and Ba^{2+}.

Declaration of interests

☒ The authors declare that they have no known competing financial interests or personal relationships that could have appeared to influence the work reported in this paper.

☐ The authors declare the following financial interests/personal relationships which may be considered as potential competing interests: